A Trans Fatty Acid Substitute Aggravates Nonalcoholic Steatohepatitis Induced in Mice by Feeding a Choline-Deficient, Methionine-Lowered, L-Amino Acid-Defined, High-Fat Diet

Noriko Suzuki-Kemuriyama
Tokyo University of Agriculture, Department of Nutritional Science and Food Safety, Faculty of Applied Bioscience
Akari Abe
Tokyo University of Agriculture, Department of Nutritional Science and Food Safety, Faculty of Applied Bioscience
Kinuko Uno
Tokyo University of Agriculture, Graduate School of Agriculture, Department of Food and Nutritional Science S
Shuji Ogawa
Tokyo University of Agriculture, Department of Nutritional Science and Food Safety, Faculty of Applied Bioscience
Atsushi Watanabe
Tokyo University of Agriculture, Department of Nutritional Science and Food Safety, Faculty of Applied Bioscience
Ryuhei Sano
Tokyo University of Agriculture, Department of Nutritional Science and Food Safety, Faculty of Applied Bioscience
Megumi Yuki
Tokyo University of Agriculture Department of Nutritional Science and Food Safety, Faculty of Applied Bioscience
Katsuhiro Miyajima
Tokyo University of Agriculture, Department of Nutritional Science and Food Safety, Faculty of Applied Bioscience
Dai Nakae (agalennde.dai@nifty.com)
Faculty of Applied Bioscience, Tokyo University of Agriculture https://orcid.org/0000-0001-5895-3830

Research

Keywords: Nonalcoholic steatohepatitis, Trans fatty acids substitutes, Choline-deficient, methionine-lowered, L-amino acid-defined, high-fat diet

Posted Date: September 21st, 2020

DOI: https://doi.org/10.21203/rs.3.rs-76235/v1

Version of Record: A version of this preprint was published on December 14th, 2020. See the published version at https://doi.org/10.1186/s12944-020-01423-3.

Abstract

Background: Nonalcoholic steatohepatitis (NASH) is a form of liver disease characterized by steatosis, necroinflammation, and fibrosis, resulting in cirrhosis and cancer. *Trans* fatty acid (TFA) is hazardous for human health and a risk factor of NASH; thus, efforts have focused on reducing its intake. However, the health benefits of reducing dietary TFA are not fully elucidated. We investigated effects of TFA and its substitute on NASH induced in mice by feeding a choline-deficient, methionine-lowered, L-amino acid-defined, high-fat diet (CDAA-HF).

Methods: Mice were fed CDAA-HF containing shortening with TFA (CDAA-HF-T(+)), CDAA-HF containing shortening with a TFA substitute (CDAA-HF-T(−)), or a control chow for 13/26 weeks.

Results: CDAA-HF-T(+) contained TFA, whereas CDAA-HF-T(−) contained no TFA and much saturated fatty acids. CDAA-HF-T(+) and CDAA-HF-T(−) induced NASH in mice, evidenced by elevated serum transaminase activity and liver changes, including steatosis, inflammation, and fibrosis. CDAA-HF-T(−) induced more hepatocellular apoptosis and proliferative (preneoplastic and non-neoplastic) nodular lesions than CDAA-HF-T(+).

Conclusions: Thus, replacement of dietary TFA with its substitute does not prevent but aggravates nutritionally induced NASH in mice, at least under the present conditions. Attention should be paid regarding future TFA substitute use in humans, and a fatty acid balance is likely more important than the particular types of fatty acids.

Background

Nonalcoholic steatohepatitis (NASH) is a form of liver disease characterized by steatosis and the death and ballooning of hepatocytes. It is also associated with inflammation and hepatic fibrosis, resulting in cirrhosis and cancer [1, 2]. It has been hypothesized that the development of NASH requires two “hits” [3]: the first hit represents the development of hepatic steatosis, and the second hit involves oxidative stress and proinflammatory cytokines, inducing further liver injury. It is also proposed that inflammation activates a stress response in hepatocytes, may lead to lipid accumulation, and can progress to steatosis in NASH [4–6]. However, growing evidence suggests that simple steatosis and NASH are two separate diseases. In this “multiple parallel hit” hypothesis, the accumulated lipotoxic/proinflammatory lipid species interact with other proinflammatory factors to promote the progression to NASH, whereas in other cases, the liver develops steatosis and remains free of inflammation [7–9]. Therefore, highly diverse processes may represent inflammatory insults, where a variety of factors are involved, including toxic lipids, nutrients, and other macrophage- and adipose-derived signals.

Recent studies suggest that the types of fat sensitize hepatocytes to inflammation [10, 11]. Recently, it has been reported that a change in the long-chain fatty acid (FA) composition via Elovl6 modulates the progress of NASH [12, 13] and that the dietary fish oils eicosapentaenoic acid (EPA, C20:5) and docosahexaenoic acid (DHA, C22:6) containing large amounts of polyunsaturated FAs (PUFAs) of the n-3 family exhibit different effects in preventing atherogenic high-fat diet-induced NASH [14].

Trans FAs (TFAs), or *trans* fats, are produced when food manufacturers add hydrogen to saturate or partially saturate the unsaturated bonds of vegetable oils for cooking, frying, or baking. The elevated intake of TFA is known to correlate to the increased incidence of coronary atherosclerotic diseases [15]. With regard to NASH, dietary exposure to TFA induces fat accumulation in the liver [16, 17]. TFA is clearly hazardous for human health; thus, the Joint WHO/FAO Expert Consultation on Diet, Nutrition, and the Prevention of Chronic Diseases (JECFA) has recommended that its intake should be reduced to less than 1% of the energy intake [18]. Hence, TFA substitutes have been developed. However, the health benefits of reducing dietary TFA are not fully understood, and the benefits and/or risks associated with the use of TFA substitutes have not been evaluated.

It is well established that a choline-deficient, methionine-lowered, L-amino acid-defined diet (CDAA) induces changes mimicking human NASH in Fischer 344 rats, such as steatohepatitis, hepatic fibrosis, liver cirrhosis, and hepatocellular carcinoma, but it exhibits only minimal effects on body weight and glucose metabolism in contrast to semi-purified methionine- and choline-deficient diets [19, 20]. Mice were largely resistant to CDAA [21], but Matsumoto et al. recently developed a modified CDAA with reduced methionine and an increased amount of fat amount by lard (CDAHFD), which effectively induced NASH in mice [22].

In this context, the aim of the present study is to comparably investigate effects of shortenings with and without TFA on NASH induced in mice by feeding our original high-fat CDAA (CDAA-HF), and to assess the safety concerns to use TFA substitutes.

Methods

Diets

As a control, a standard laboratory control chow (composed of 60% carbohydrate, 13% fat, and 27% protein on a caloric basis) was obtained from Oriental Yeast Co., Ltd. (Tokyo, Japan). As experimental diets, CDAA-HF-T(+) (the fat amount 45 kcal% by shortening with TFA, Primex®, and the methionine amount 0.1%; ID A16032901) and CDAA-HF-T(−) (the fat amount 45 kcal% by shortening without TFA, Primex Z®, and the methionine amount 0.1%; ID A16032902) were made-to-order products of Research Diet Inc. (New Brunswick, NJ). The dietary component of each diet is shown in Additional file 1. It should be emphasized that CDAA-HF is different from CDAHFD. Notably, the fat and methionine amounts of CDAA are 31 kcal% and 0.17% [19, 20], whereas those of CDAHFD are 60 kcal% and 0.1% [22], respectively. The diets were frozen until use and changed every other day to prevent the formation of oxidized products.

Animals

Five-week-old male C57BL/6J mice were purchased from Japan SLC (Shizuoka, Japan) and adapted to the environment for a week prior to the study. Mice were housed under temperature-controlled conditions (22 °C on average) in colony cages with a 12-h light/12-h dark cycle and were given free access to food and water. At 6 weeks of age, mice were randomly assigned to three groups that were fed the control chow, CDAA-HF-T(+), or CDAA-HF-T(−) for 13 or 26 weeks during which body weight, food consumption, and water intake were weekly monitored. At the end of the experimental periods, blood samples were collected from the tail vein of all mice in a non-fasting state, and mice were sacrificed by exsanguination under light isoflurane anesthesia in the early light phase. During the autopsy, all organs were carefully observed, and the liver and organs with lesions were excised and weighed.

Histological analysis

Liver samples were fixed in 10% neutrally buffered formalin, embedded in paraffin, and cut into 4-μm-thick sections for hematoxylin–eosin (H&E) and Sirius Red staining. For Sirius Red staining, the area of fibrosis was measured using cellSens Dimension software (Olympus, Tokyo, Japan) by a scientist blinded to the treatment of the mice. The histopathological evaluation of hepatocellular proliferative lesions was performed according to the International Harmonization of Nomenclature and Diagnostic Criteria (INHAND) [23]. Briefly, the diagnostic criteria were as follows: regenerative hepatocellular hyperplasia, lesions spanning several hepatic lobules where portal triads and central veins are present, and hepatocellular adenoma, lesions that are greater than several lobules and have no portal triads or central veins. The findings and diagnoses were peer-reviewed by a board-certified toxicologic pathologist who was not one of the co-authors to improve the quality of the pathology data. Immunohistochemical analyses were performed as previously described [24] with samples obtained from mice treated for 13 or 26 weeks using the following primary antibodies: rat anti-mouse monoclonal antibody for F4/80 as a marker of macrophages (1:200; Abcam, Cambridge, UK), rabbit antihuman polyclonal antibody for α-smooth muscle actin (α-SMA) as a marker of activated hepatic stellate cells (1:200; Abcam, Cambridge, UK), and mouse antihuman monoclonal antibody for cytokeratin 8/18 (CK8/18) as a marker of putative hepatocellular preneoplastic lesions (1:500; Developmental Studies Hybridoma Bank, Iowa, USA). The visualization of antibody binding was performed using a Histofine Simple Stain Kit (Nichirei Corp., Tokyo, Japan) for F4/80 and α-SMA or a VectaStain Elite ABC Kit (Vector Laboratories, Burlingame, CA, USA) for CK8/18. All sections were counterstained with hematoxylin and histopathologically examined in a blinded manner, and the findings were graded from normal (1) to severe (4). The numbers of CK8/18-positive putative hepatocellular preneoplastic lesions consisting of 1, 2, 3, or more cells were counted per ten light microscopic fields (× 200).

Plasma and hepatic chemistries

Plasma was prepared from blood samples to measure triglyceride (TG) and total cholesterol (TC) concentrations and alanine aminotransferase (ALT) activity using an automatic analyzer (DRI-CHEM; Fujifilm, Tokyo, Japan) or colorimetry test kits purchased from Wako Pure Chemical Industries (Osaka, Japan). Hepatic TG and TC levels were measured as previously described [25].

FA compositions of diets and livers

The FA composition was quantitatively measured by reversed-phase high-performance liquid chromatography coupled with Fourier transform mass spectrometry (LC/FTMS), as previously reported [26]. Briefly, lipid extraction from samples was performed by bead mill homogenization in 1 mL of methanol. The samples were then mixed by constant shaking (Multi Shaker, Tokyo Rikakikai Co., Ltd.) and centrifuged at 15,000 rpm for 5 min. The obtained supernatant was then collected as the lipid extract. This lipid extract was saponified in 0.5 mol/L potassium hydroxide in ethanol/water (96/4, v/v). The reaction was terminated by adding 1 mol/L hydrochloric acid until the solution became acidic, hexane (100 μL) was added, and the solution was mixed by stirring. The mixture was centrifuged, and the upper layer was collected. After evaporation, the residue was dissolved in 100 ng/mL $^{18}O_2$ containing methanol and used for LC/FTMS analysis. LC was performed using an LC-20ADXR ternary pump system equipped with a DGU-20A5R degassing unit, SIL-20AC autosampler, and CTO-20AC column oven (Shimadzu Co., Ltd., Kyoto, Japan). The LC system was coupled with an LTQ Orbitrap XL hybrid linear ion trap–Fourier transform mass spectrometer (Thermo Fisher Scientific, Waltham, MA, USA). FTMS detection was conducted in a full scan mode at a resolution of 30000 and a range of m/z 140–600. FAs were detected by obtaining the extracted ion chromatograms of deprotonated ions ([M-H]-) at a mass tolerance of 10 ppm. Instrument control, data acquisition, and data processing were performed using Xcalibur 2.1.0 software (Thermo Fisher Scientific).

RNA extraction and analysis

Total RNA was extracted from the liver using a Sepasol reagent (Nacalai Tesque, Kyoto, Japan) and was reverse-transcribed using a PrimeScript RT Master Kit (Takara Bio Inc., Shiga, Japan), according to the manufacturers' instructions. Then, quantitative real-time PCR (qPCR) was performed using a SYBR Premix Ex Taq (Takara Bio Inc. Shiga, Japan) and specific primer sets with a Thermal Cycler Dice Real-Time System Single (Takara Bio Inc. Shiga, Japan). The primer sequences for qPCR in this study are shown in Additional file 2. The mRNA expression levels were normalized to those of cyclophilin mRNA. Portions of the RNA samples were subjected to RNA sequencing (RNA-Seq) and corresponding qPCR analyses. RNA-Seq was performed as previously described [27]. Portions of the 100 ng of total RNA from the livers of the control, CDAA-HF-T(+), and CDAA-HF-T(−) groups (treated for 13 weeks, n = 3–4) were used for library preparation. Sequencing libraries were generated using a TruSeq RNA Library Preparation Kit v2 (Illumina Inc., San Diego, CA, USA). The principal component analysis (PCA), differential expression analysis, generation of heat maps with hierarchical clustering of samples, and features and functional annotation analyses using Ingenuity Pathway Analysis (IPA) software (Ingenuity Systems, Qiagen Co., Ltd.) were performed as previously described [27].

Immunoblotting

Immunoblotting was performed as previously described [25]. Aliquots of 50 μg of total protein lysates extracted from the livers were subjected to 10% sodium dodecyl sulfate–polyacrylamide gel electrophoresis and transferred to polyvinylidene fluoride membranes (Millipore, Darmstadt, Germany). The membranes were probed with anti-glyceraldehyde 3-phosphate dehydrogenase (GAPDH, Santa Cruz Biotechnology, Dallas, USA), cleaved caspase 3, phospho-nuclear factor (NF)κB, and IκB (Cell Signaling

Technology, Denver, USA) antibodies followed by horseradish peroxidase (HRP)-conjugated anti-mouse or rabbit IgG secondary antibodies (Cell Signaling Technology, Denver, USA). Immune complexes were visualized using enhanced chemiluminescence (Bio-Rad, Richmond, CA).

Statistical analysis

Numeral values were expressed as means ± standard deviations (SDs). Analysis of variance (ANOVA) followed by the Tukey–Kramer test was used to assess differences among groups. Differences were considered significant at $p < 0.05$.

Results

Dietary and hepatic FA compositions

Dietary FA compositions are shown in Table 1. Compared to the control chow, CDAA-HF-T(+) and CDAA-HF-T(−) contained higher percentages of saturated and monounsaturated FAs, whereas the proportions of n-6 and n-3 polyunsaturated FAs were reduced. The ratio of saturated FAs is particularly higher in CDAA-HF-T(−) than in CDAA-HF-T(+), mainly due to the increase in palmitic acid (C16:0). However, not surprisingly, CDAA-HF-T(+) contained more TFAs.

Table 1
Dietary FA compositions

Ingredient (%)	Control chow	CDAA-HF-T(+)	CDAA-HF-T(−)
C14:0	0.5	0.3	0.8
C16:0	11.4	13.2	26.1
C16:1 n-7	0.7	0.1	0.2
C18:0	1.1	6.0	4.2
C18:1 n-7	1.6	10.6	0.9
C18:1 n-7 t	0.1	7.2	0.0
C18:1 n-9	23.2	32.6	43.0
C18:1 n-9 t	0.1	3.4	0.1
C18:2 n-6	52.1	25.0	23.8
C18:2 n-6 tt	N.D.	0.6	0.0
C18:3 n-3	3.4	0.4	0.4
C18:3 n-6	N.D.	0.2	0.1
C20:0	0.3	0.4	0.4
C20:2 n-6	0.0	0.0	0.0
C20:3 n-6	N.D.	N.D.	N.D.
C20:4 n-6	N.D.	0.0	N.D.
C20:5 n-3	1.2	N.D.	N.D.
C22:5 n-3	0.1	N.D.	N.D.
C22:6 n-3	4.2	N.D.	N.D.
Total	100	100	100

Ingredient (%)	Control chow	CDAA-HF-T(+)	CDAA-HF-T(−)
SFA	13.2	19.9	31.5
MUFA	25.5	43.3	44.0
n-6 PUFA	52.2	25.1	23.9
n-3 PUFA	8.9	0.4	0.4
TFA	0.2	11.2	0.2

N.D.; not detected.

Hepatic FA compositions at the end of week 26 are shown in Table 2. The livers of mice fed CDAA-HF-T(+) significantly contained more *cis*-vaccenic (C18:1 n-7), *trans*-vaccenic (C18:1 n-7 t), and elaidic acid (C18:1 n-9 t) than those fed CDAA-HF-T(−). Linolelaidic acid (C18:2 n-6, 9 tt) was only detected in the livers of mice fed CDAA-HF-T(+). Furthermore, the livers of mice fed CDAA-HF-T(−) significantly contained higher amounts of γ-linolenic (C18:3 n-6), dihomo-γ-linolenic (C20:3 n-6), and arachidonic acid (C20:4 n-6) than those of mice fed CDAA-HF-T(+), but the amount of linoleic acid (C18:2 n-6) was similar in the livers of mice fed either CDAA-HF-T(+) or CDAA-HF-T(−).

Table 2
Hepatic FA compositions at the end of week 26

Ingredient (ng/mg)	Control chow	CDAA-HF-T(+)	CDAA-HF-T(−)
C14:0	120 ± 21	1131 ± 192 *	1021 ± 140 *
C16:0	5423 ± 715	27503 ± 4477 *	30389 ± 5932 *
C16:1n-7	933 ± 268	4856 ± 1258 *	4165 ± 587 *
C18:0	1984 ± 417	3671 ± 291 *	4479 ± 1021 *
C18:1n-7	830 ± 207	10380 ± 1441 *	4237 ± 414 *
C18:1n-7t	16 ± 5	2246 ± 315 *	96 ± 15 *, +
C18:1n-9	4860 ± 898	66045 ± 12407 *	83732 ± 19926 *
C18:1n-9t	13 ± 7	1647 ± 156 *	155 ± 44 +
C18:2n-6	7692 ± 1247	35212 ± 1832 *	33790 ± 8871 *
C18:2n-6tt	N.D.	901 ± 63	22 ± 7
C18:3n-3	177 ± 55	154 ± 20	124 ± 40
C18:3n-6	50 ± 32	1393 ± 157 *	2517 ± 73 *, +
C20:0	51 ± 22	169 ± 16 *	224 ± 51 *
C20:2n-6	67 ± 11	433 ± 56 *	354 ± 52 *
C20:3n-6	443 ± 62	1404 ± 89 *	2158 ± 470 *, +
C20:4n-6	2889 ± 434	8668 ± 775 *	12602 ± 3034 *, +
C20:5n-3	400 ± 91	11 ± 1 *	27 ± 13 *
C22:5n-3	148 ± 26	178 ± 17	219 ± 47 *
C22:6n-3	8754 ± 15	2930 ± 476 *	4184 ± 1178 *
Total	34850 ± 4687	168925 ± 20918 *	184484 ± 41347 *

Values are represented as mean ± SD, n = 4.

Significantly different from the values of *control chow or +CDAA-HF-T(+) groups.

N.D.; not detected.

Organ weights and plasma and hepatic chemistries

Organ weights and plasma and hepatic chemistries at the end of week 13 are shown in Table 3. CDAA-HF, either with or without shortening containing TFA, decreased body weight, increased the absolute and relative weights of the liver and eWAT, and enhanced plasma ALT activity than the control chow. Although not significant, plasma TG and TC levels were decreased, whereas their hepatic levels were markedly elevated in these groups. However, there were no significant differences in these parameters between CDAA-HF-T(+) and CDAA-HF-T(−) groups.

Table 3
Organ weights and plasma and hepatic chemistries at the end of week 13

	Control chow	**CDAA-HF-T(+)**	**CDAA-HF-T−-)**
Body weight	26.32 ± 1.71	23.72 ± 1.46*	22.94 ± 0.99*
Liver (g)	1.36 ± 0.06	1.75 ± 0.30*	1.76 ± 0.25*
Liver/BW (%)	4.85 ± 0.14	7.38 ± 0.83*	7.47 ± 0.86*
Kidney (g)	0.36 ± 0.04	0.31 ± 0.06	0.27 ± 0.04*
Heart (g)	0.17 ± 0.05	0.15 ± 0.06	0.12 ± 0.02
eWAT (g)	0.43 ± 0.11	0.60 ± 0.07*	0.51 ± 0.03
eWAT/BW (%)	1.58 ± 0.40	2.53 ± 0.23*	2.19 ± 0.19*
TG (mg/dL)	169.13 ± 43.18	106.03 ± 10.51*	110.34 ± 10.45*
TC (mg/dL)	138.71 ± 22.95	101.46 ± 37.72	91.21 ± 8.75
ALT (IU/L)	23.63 ± 0.81	74.26 ± 12.31*	83.58 ± 18.62*
Liver TG (mg/g)	6.17 ± 3.33	57.91 ± 25.26*	58.93 ± 12.78*
Liver TC (mg/g)	2.42 ± 0.49	3.53 ± 0.45*	3.21 ± 0.26*

Values are represented as mean ± SD, n = 4–5.

eWAT, epididymal white adipose tissue; TC, total cholesterol; TG, triglyceride.

*Significantly different from the control value.

Nonproliferative liver lesions

The representative microscopic features of non-proliferative liver lesions and their gradings are shown in Fig. 1. At the end of week 13, macrovesicular steatosis characterized by hepatocytes with a single cytoplasmic large vacuole was observed in almost all hepatocytes in the CDAA-HF groups. Furthermore, inflammatory clusters where Kupffer cells and hypertrophied macrophages and the number of activated stellate cells were markedly accumulated were observed in these groups, as demonstrated by the immunohistochemical staining of the macrophage marker F4/80 and α-SMA, respectively. In addition, Sirius Red staining revealed fibrosis in the CDAA-HF groups. While the magnitudes of fatty changes and fibrosis were similar within these groups, the inflammation-related changes were only slightly greater in CDAA-HF-T(−) mice than in CDAA-HF-T(+) mice.

At the end of week 26, while steatosis and inflammation remained unchanged, hepatic fibrosis continuously progressed in the CDAA-HF groups (see Additional file 3).

Proliferative liver lesions at the end of week 26

At the end of week 26 in CDAA-HF groups, rough surfaces and nodules were macroscopically observed in the liver (Fig. 2a), which corresponded to the microscopical identification of hepatocellular proliferative lesions (Fig. 2b). The proliferative characteristics of the lesions were evidenced by the high proliferating cell nuclear antigen (PCNA) -positive index, which were 0.04, 4.47, 1.37 and 1.04% in normal liver tissue of control animals, proliferative liver lesions of CDAAHF-T(-), adjacent nonproliferative liver tissue of CDAA-HF-T(-) and liver tissue of CDAA-HF-T(+), respectively (data not shown). The foci of cellular alteration are proliferative lesions, including putatively preneoplastic lesions, which were observed in 1/11 mice (9%) and 10/10 mice (100%) in CDAA-HF-T(+) and CDAA-HF-T(−) groups, respectively. Regenerative hepatocellular hyperplasia lesions are proliferative but not preneoplastic [23] and were observed in 1/11 mice (9%) and 3/10 mice (30%) in CDAA-HF-T(+) and CDAA-HF-T(−) groups, respectively.

The number of hepatocytes immunohistochemically positive for CK8/18, a marker for preneoplastic hepatocellular lesions [29], was increased in CDAA-HF groups, among which the number was higher in the CDAA-HF-T(−) group than in the CDAA-HF-T(+) group (Fig. 2c).

Table 4
Incidences of hepatocellular proliferative lesions at the end of week 26

Lesion	Control chow	CDAA-HF-T(+)	CDAA-HF-T(−)
Foci of celullar alteration	0 (0)	1 (9)	10 (100)
Hyperplasia, hepatocellular, regenerative	0 (0)	1 (9)	3 (30)

n = 10−11.

Gene expression profiles

The RNA sequencing analysis was performed using liver samples obtained at the end of week 13. To identify outlier samples for quality control and determine the primary causes of variation in the dataset, PCA was conducted (Fig. 3a). The control chow and CDAA-HF groups were separated by the first principal component (42.4%, horizontal axis). Then, the second principal component (19.8%, vertical axis) separated CDAA-HF-T(+) and CDAA-HF-T(−) groups. The analyses of various differentially expressed genes (DEGs) were performed between the control chow and either CDAA-HF-T(+) or CDAA-HF-T(−) under the conditions of a false discovery rate (FDR) p value < 0.05 and fold change (FC) > ± 1.5. The comparison between CDAA-HF-T(+) and CDAA-HF-T(−) groups was conducted with an FDR p value < 0.05. The Venn diagram of these genes is shown in Fig. 3b. The specific DEGs called for the control chow versus CDAA-

HF-T(+) groups, the control chow versus CDAA-HF-T(−), and CDAA-HF-T(+) versus CDAA-HF-T(−) were 1,280, 539, and 13, respectively.

Pathway analysis and hepatic status of apoptosis and NF-κB signaling

The activation states of diseases and functions were predicted according to the functional analysis of the DEGs using IPA. The activation z-score > 2 of CDAA-HF-T(+) versus the control chow, CDAA-HF-T(−) versus the control chow, and CDAA-HF-T(−) versus CDAA-HF-T(+) were shown in Fig. 4a. In the CDAA-HF-T(−) group, genes related to cell death, such as organismal death and mortality, were overexpressed. In contrast, genes related to the immune system, such as lymphopoiesis and the homeostasis of leukocytes, were overexpressed in the CDAA-HF-T(+) group. The selected signaling pathways by IPA analysis were listed in Additional file 4.

Fledstein et al. found that the expression of active caspase 3 in NASH specimens was strongly correlated with apoptosis in hepatocytes and the progression of NASH [30]. The level of cleaved (thereby activated) caspase 3 protein was greatly increased in the CDAA-HF-T(−) group, whereas the magnitude of this change was not significant in the CDAA-HF-T(+) group (Fig. 4b).

NF-κB mediates both proinflammatory and antiapoptotic responses, thereby protecting hepatocytes from cell death when inflammatory and immune responses are initiated. Therefore, NF-κB signaling makes an essential contribution to liver homeostasis and wound-healing processes [31]. NF-κB phosphorylation (activation) was greatly attenuated in the CDAA-HF-T(−) group, whereas the magnitude of this change was only moderate in the CDAA-HF-T(+) group (Fig. 4b). Furthermore, the protein level of IκBα tended to increase in CDAA-HF groups.

Sulfotransferase family 1E member 1 (SULT1E1) and insulin-like growth factor (IGF)-1 expression levels

Using the genes selected by the expression analysis, the clustering of individual mice (horizontal axis) and information between genes (vertical axis) was conducted to generate a heat map (Fig. 5a). The results indicated that these clusters were divided in the control chow, CDAA-HF-T(+), and CDAA-HF-T(−) groups. According to the heat map, genes overexpressed or downregulated only in the CDAA-HF-T(−) group were further explored. Four genes were identified to be overexpressed in the CDAA-HF-T(−) group. Among them, qPCR revealed that the mRNA expression of the *SULT1E1* gene (Fig. 5b) was markedly increased in the CDAA-HF-T(−) group. In the immunoblot analysis, the strongest band of SULT1E1 was detected near 35 kDa in the CDAA-HF-T(−) group. In contrast, two weak bands were detected in the control chow group (Fig. 5c). It has been reported that enhanced SULT1E1 activity may play a role in inhibiting growth hormone (GH)-stimulated IGF-1 synthesis via the sulfation and inactivation of β-estradiol (E2) [32]. The *IGF-1* gene tended to be downregulated in the CDAA-HF-T(−) group at the end of week 13, and its expression was further and significantly decreased at the end of week 26 (Fig. 5d).

Discussion

This study aimed to determine whether TFA and its substitute have different effects on CDAA-HF diet-induced NASH in mice. While basic outcomes were similar in the livers of mice fed CDAA-HF containing either TFA or its substitute, the proliferative liver lesions were more substantial in the CDAA-HF-T(−) group than in the CDAA-HF-T(+) group. It is suggested that this increased hepatotoxicity in CDAA-HF-T(−) mice is due to the proapoptotic hepatic microenvironment at a relatively early stage.

The toxic effects of excess lipids, known as lipotoxicity, have recently been identified to cause hepatocellular damage and chronic inflammation in the liver and to be one of the major causes of NASH [33, 34]. The major determinant of lipotoxicity for NASH is not the total amount of TG stored in hepatocytes, but it is the specific class of lipids that damages hepatocytes [33, 34]. Growing evidence suggests that TFA aggravates nonalcoholic fatty liver disease (NAFLD) and NASH. For instance, oil containing a large amount of TFA promotes liver steatosis and injury through the enhancement of lipid synthesis, hepatocellular necrosis and apoptosis, and cytokine secretion from Kupffer cells [16, 17, 35]. In the present study, while CDAA-HF-T(+) and CDAA-HF-T(−) equally caused the accumulation of hepatic lipid content, inflammatory and fibrotic changes (represented by F4/80 and α-SMA scores, respectively) were only slightly greater in the CDAA-HF-T(−) group than in the CDAA-HF-T(+) group at the end of week 13. At the end of week 26, more hepatocellular proliferative lesions, either preneoplastic or non-neoplastic, had developed in the CDAA-HF-T(−) group than in the CDAA-HF-T(+) group. Therefore, CDAA-HF-T(−) may exhibit more severe toxic and possibly carcinogenic effects in the liver of mice than CDAA-HF-T(+), which is likely not simply due to the quantitative difference in dietary or hepatic lipids but to the qualitative difference caused by the absence and presence of TFA.

It has been proposed that hepatic FA composition is an important determinant of NASH progression [12, 13, 36, 37]. Arachidonic acid-derived prostaglandins and related lipid metabolites are active mediators of inflammation [38–40]. In addition to oxidative stress, cyclooxygenase (COX) 2 activity and prostaglandin (PG)E_2 content are the major factors involved in the mechanisms underlying hepatotoxicity and hepatocarcinogenicity in rats fed CDAA [41]. Compared with the CDAA-HF-T(+) group, the CDAA-HF-T(−) group showed a significant increase in γ-linolenic (C18:3 n-6), dihomo-γ-linolenic (C20:3 n-6), and arachidonic acid (C20:4 n-6) but no change in linoleic acid (C18:2 n-6) in the liver. These results suggest that CDAA-HF-T(−) may promote liver injury by upregulating n-6 PUFA synthesis and metabolism more progressively than CDAA-HF-T(+).

Accumulating evidence indicates that TFA is a risk factor of NASH in animals [16, 42]. For instance, in low-density lipoprotein (LDL) receptor-knockout weaning male mice fed a 16-week high-fat diet (40% of energy as fat) enriched with TFA (especially elaidic acid (C18:1 n-9 t)), the development of NASH is more severe. Specifically, more histopathological liver lesions characterized by macrovesicular steatosis and inflammatory cell infiltration were observed compared with mice fed similarly high-fat diets enriched with PUFAs (especially linoleic acid (C18:2 n-6)) or saturated FAs (SFA) (especially palmitic acid (C16:0)), which induced only mild microvesicular hepatic steatosis and minimal inflammation [17]. However, in the present study, CDAA-HF-T(−) containing a high amount of palmitic acid caused greater NASH-like hepatotoxicity (and possibly hepatocarcinogenicity) than CDAA-HF-T(+) containing TFAs, such as *trans*-vaccenic (C18:1 n-7 t) and elaidic acid in association with *cis*-vaccenic acid (C18:1 n-7). One possible explanation is that SFAs may be associated with a higher risk of NASH than TFAs. In a recent study using a Western diet mouse model of steatohepatitis, a stronger induction of proinflammatory cytokines and collagen accumulation was observed when non-trans fats were used as a fat source compared with the use of trans fat or corn oil [43]. It has been reported that vaccenic acid (C18:1 n-7 t), a predominant ruminant-derived TFA in the food chain, ameliorates hyperlipidemia and the NAFLD activity score [44]. In contrast, palmitate itself is known to induce hepatic injury [45]. Furthermore, in the LDL receptor-knockout male mice, CDAA modified by including 1% cholesterol and 41% palm oil, containing a high amount of palmitate, induces NASH and hepatocellular carcinomas within 39 weeks [46]. This indicates that progression of steatohepatitis is not important for particular types of FAs, such as TFA but is important for comprehensive toxic or protective FAs balance.

RNA sequencing revealed that genes involved in cell death, such as organismal death and mortality, were overexpressed in the CDAA-HF-T(−) group. Cell death, including apoptosis, is essential in the progression of NAFLD and NASH and correlates with progressive inflammation and fibrosis [47]. While both CDAA-HF-T(+) and CDAA-HF-T(−) induced hepatocellular apoptosis, the effect of CDAA-HF-T(−) was more substantial than CDAA-HF-T(+). Similarly, both CDAA-HF-T(+) and CDAA-HF-T(−) reduced NF-κB phosphorylation, but the effect of CDAA-HF-T(−) was greater than CDAA-HF-T(+). Together, these results suggest that the increased hepatotoxicity of CDAA-HF-T(−) is due to the more proapoptotic hepatic microenvironment partially introduced by the inhibition of NFκB phosphorylation. In fact, Luedde proposed that NF-κB acts as a central link between hepatic injury, fibrosis, and hepatocellular carcinoma and that it may serve as a target for their prevention and treatment [31]. Nevertheless, NF-κB can act as a double-edged sword, and the inhibition of NF-κB may not necessarily exert beneficial effects and can potentially negatively impact on hepatocyte viability [48].

The mRNA expression of the *SULT1E1* gene was specifically increased in the CDAA-HF-T(−) group. In addition, SULT1E1 protein was detected by Western blotting analysis and immunohistochemically detected in hepatocytes. The *SULT1E1* gene encodes sulfotransferase family E1 that is responsible for the sulfation and inactivation of E2 [49]. It has previously been reported that SULT1E1 is expressed in hepatocytes, and its activity was significantly elevated in the livers of cystic fibrosis-associated liver disease model mice [50, 51]. SULT1E1 expression is also enhanced in the case of NASH induced in IKKβ-deficient male mice fed a high cholesterol and SFA diet, suggesting that IKKβ plays a protective role in the hepatocytes of these mice partly by its ability to repress SULT1E1 [52]. In the present study, the SULT1E1 protein band was detected at a lower position in the CDAA groups than in the control chow group. We also confirmed in other experiments that SULT1E1 protein was detected at a lower level in severe NASH than in the control chow group (data not shown). These results suggest that structural changes to the protein may occur in association with the development of NASH. This change in the SULT1E1 protein may be a cause or result of the events occurring throughout the course of NASH. In either case, this change likely has important implications in the underlying molecular mechanisms of NASH and thus can serve as a potential target to control the disease. However, further studies are required to test these possibilities. The enhanced SULT1E1 activity may also inhibit GH-stimulated STAT5b phosphorylation and IGF-1 synthesis via the sulfation and inactivation of E2 [32]. In fact, the *IGF-1* gene was downregulated in the CDAA-HF-T(−) group. GH and IGF-I coordinately play essential roles in the liver [53]. They are thought to be molecular targets for the treatment of NASH and/or cirrhosis [54–56]. Thus, elevated SULT1E1 may negatively regulate IGF-1 synthesis and thereby GH signaling, contributing to the progression of NASH. Further studies are required to elucidate the detailed pathway or mechanism.

Conclusions

In conclusion, the replacement of dietary TFA with its substitute does not prevent but rather aggravates nutritionally induced NASH in mice, at least under the present conditions. This aggravation may be because the shortening with TFA substitute contained more toxic fatty acids compared with the shortening with TFA. Attention should thus be paid regarding future TFA substitute use in humans, and the FA balance is likely more important than the presence of particular types of FAs, such as TFA and SFA.

On the other hand, it is suggested that the aggravation of NASH in the CDAA-HF-T(−) group may be do to the proapoptotic hepatic microenvironment, introduced by the partial inhibition of the NFκB phosphorylation and the overexpression of SULTE1E1. These factors can serve as novel molecular targets for the prevention and/or treatment of NASH.

List Of Abbreviations

ANOVA Analysis of variance

DEG Differentially expressed genes

FA Fatty acid

FDR False discovery rate

GH Growth hormone

IPA Ingenuity Pathway Analysis

LDL Low-density lipoprotein

NAFLD Non-alcoholic fatty liver disease

PCA Principal component analysis

SD Standard deviations

TC Total cholesterol

TFA Trans fatty acid

Declarations

Ethics approval and consent to participate

All animal husbandry and experiments were performed in compliance with the guiding principle of the Tokyo University of Agriculture and approved by the Animal Experiment Committee of the Tokyo University of Agriculture. Consequently, the present study has obeyed all related domestic and international laws, regulations, and guidelines. In particular, animal experiments conducted in the present study complied with the ARRIVE guidelines and were carried out in accordance with the UK Animals (Scientific Procedures) Act, 1986 and associated guidelines, EU Directive 2010/63/EU for animal experiments, or the National Institutes of Health guide for the care and use of laboratory animals (NIH Publications No. 8023, revised 1978).

Consent for publication

Not applicable.

Availability of data and materials

Not applicable.

Competing interests

Not applicable.

Funding

The present study was supported in part by the Grant-in-Aid for Young Scientists (19K20124), research grant from The Japan Food Chemical Research Foundation (H30-006), MEXT-Supported Program for the Strategic Research Foundation at Private Universities, 2013–2017 (S1311017) from the Ministry of Education, Culture, Sports, Science and Technology of Japan and the research budget of the Tokyo University of Agriculture.

Authors' contributions

N.K. designed the project; N.K., A.A., and K.U. performed experiments; S.O., R.S. and A.W. contributed analysis tools; N.K., A.A., K.U., S.O., M.Y., K.M. and D.N. analyzed and interpreted data; and N.K. and D.N. prepared the manuscript. All authors reviewed the manuscript.

Acknowledgements

The authors are grateful for technical support and scientific suggestion of Dr. Hironobu Uchiyama, Genome Research Center, Tokyo University of Agriculture, Tokyo, Japan (his affiliation at the time when the present study was conducted). The authors thank Kaori Ikehata, Takuya Yamashita, Satomi Uchino and Syunta Sato for their technical support. They also thank members of our laboratories other than the present co-authors for discussion and helpful comments.

References

1. Angulo P. Nonalcoholic fatty liver disease. N Engl J Med. 2002;346:1221-31. Epub 2002/04/19. doi:10.1056/NEJMra011775. PubMed PMID: 11961152.
2. Farrell GC, Larter CZ. Nonalcoholic fatty liver disease: from steatosis to cirrhosis. Hepatology. 2006;43:S99-112. Epub 2006/02/01. doi:10.1002/hep.20973. PubMed PMID: 16447287.
3. Day CP, James OF. Steatohepatitis: a tale of two "hits"? Gastroenterology. 1998;114:842-5. Epub 1998/04/18. PubMed PMID: 9547102.
4. Li Z, Yang S, Lin H, Huang J, Watkins PA, Moser AB, et al. Probiotics and antibodies to TNF inhibit inflammatory activity and improve nonalcoholic fatty liver disease. Hepatology. 2003;37:343-50. Epub 2003/01/24. doi:10.1053/jhep.2003.50048. PubMed PMID: 12540784.
5. Lee AH, Scapa EF, Cohen DE, Glimcher LH. Regulation of hepatic lipogenesis by the transcription factor XBP1. Science. 2008;320:1492-6. Epub 2008/06/17. doi:10.1126/science.1158042. PubMed PMID: 18556558; PubMed Central PMCID: PMCPMC3620093.
6. Obstfeld AE, Sugaru E, Thearle M, Francisco AM, Gayet C, Ginsberg HN, et al. C-C chemokine receptor 2 (CCR2) regulates the hepatic recruitment of myeloid cells that promote obesity-induced hepatic steatosis. Diabetes. 2010;59:916-25. Epub 2010/01/28. doi:10.2337/db09-1403. PubMed PMID: 20103702; PubMed Central PMCID: PMCPMC2844839.
7. Neuschwander-Tetri BA. Hepatic lipotoxicity and the pathogenesis of nonalcoholic steatohepatitis: the central role of nontriglyceride fatty acid metabolites. Hepatology. 2010;52:774-88. Epub 2010/08/05. doi:10.1002/hep.23719. PubMed PMID: 20683968.
8. Tilg H, Moschen AR. Evolution of inflammation in nonalcoholic fatty liver disease: the multiple parallel hits hypothesis. Hepatology. 2010;52:1836-46. Epub 2010/11/03. doi:10.1002/hep.24001. PubMed PMID: 21038418.
9. Buzzetti E, Pinzani M, Tsochatzis EA. The multiple-hit pathogenesis of non-alcoholic fatty liver disease (NAFLD). Metabolism. 2016;65:1038-48. Epub 2016/01/30. doi:10.1016/j.metabol.2015.12.012. PubMed PMID: 26823198.
10. Zambo V, Simon-Szabo L, Szelenyi P, Kereszturi E, Banhegyi G, Csala M. Lipotoxicity in the liver. World J Hepatol. 2013;5:550-7. Epub 2013/11/02. doi:10.4254/wjh.v5.i10.550. PubMed PMID: 24179614; PubMed Central PMCID: PMCPMC3812457.
11. Marra F, Svegliati-Baroni G. Lipotoxicity and the gut-liver axis in NASH pathogenesis. J Hepatol. 2018;68:280-95. Epub 2017/11/21. doi:10.1016/j.jhep.2017.11.014. PubMed PMID: 29154964.

12. Kuba M, Matsuzaka T, Matsumori R, Saito R, Kaga N, Taka H, et al. Absence of Elovl6 attenuates steatohepatitis but promotes gallstone formation in a lithogenic diet-fed Ldlr(-/-) mouse model. Sci Rep. 2015;5:17604. Epub 2015/12/02. doi:10.1038/srep17604. PubMed PMID: 26619823; PubMed Central PMCID: PMCPMC4664962.
13. Matsuzaka T, Atsumi A, Matsumori R, Nie T, Shinozaki H, Suzuki-Kemuriyama N, et al. Elovl6 promotes nonalcoholic steatohepatitis. Hepatology. 2012;56:2199-208. Epub 2012/07/04. doi:10.1002/hep.25932. PubMed PMID: 22753171.
14. Suzuki-Kemuriyama N, Matsuzaka T, Kuba M, Ohno H, Han SI, Takeuchi Y, et al. Different effects of eicosapentaenoic and docosahexaenoic acids on atherogenic high-fat diet-induced non-alcoholic fatty liver disease in mice. PloS one. 2016;11:e0157580. Epub 2016/06/23. doi:10.1371/journal.pone.0157580. PubMed PMID: 27333187; PubMed Central PMCID: PMCPMC4917109.
15. Mozaffarian D, Katan MB, Ascherio A, Stampfer MJ, Willett WC. Trans fatty acids and cardiovascular disease. N Engl J Med. 2006;354:1601-13. Epub 2006/04/14. doi:10.1056/NEJMra054035. PubMed PMID: 16611951.
16. Obara N, Fukushima K, Ueno Y, Wakui Y, Kimura O, Tamai K, et al. Possible involvement and the mechanisms of excess trans-fatty acid consumption in severe NAFLD in mice. J Hepatol. 2010;53:326-34. Epub 2010/05/14. doi:10.1016/j.jhep.2010.02.029. PubMed PMID: 20462650.
17. Machado RM, Stefano JT, Oliveira CPMS, Mello ES, Ferreira FD, Nunes VS, et al. Intake of trans fatty acids causes nonalcoholic steatohepatitis and reduces adipose tissue fat content. J Nutr. 2010;140:1127-32. doi:10.3945/jn.109.117937.
18. Diet, nutrition and the prevention of chronic diseases. World Health Organ Tech Rep Ser. 2003;916:i-viii, 1-149, backcover. Epub 2003/05/29. PubMed PMID: 12768890.
19. Nakae D, Yoshiji H, Mizumoto Y, Horiguchi K, Shiraiwa K, Tamura K, et al. High incidence of hepatocellular carcinomas induced by a choline deficient L-amino acid defined diet in rats. Cancer Res. 1992;52:5042-5.
20. Nakae D, Yoshiji H, Maruyama H, Kinugasa T, Denda A, Konishi Y. Production of both 8-hydroxydeoxyguanosine in liver DNA and γ-glutamyltransferase-positive hepatocellular lesions in rats given a choline-deficient, l-amino acid-defined diet. Jpn J Cancer Res. 1990;81:1081-4. doi:10.1111/j.1349-7006.1990.tb02515.x.
21. Denda A, Kitayama W, Kishida H, Murata N, Tsutsumi M, Tsujiuchi T, et al. Development of hepatocellular adenomas and carcinomas associated with fibrosis in C57BL/6J male mice given a choline-deficient, L-amino acid-defined diet. Jpn J Cancer Res. 2002;93:125-32. doi:10.1111/j.1349-7006.2002.tb01250.x.
22. Matsumoto M, Hada N, Sakamaki Y, Uno A, Shiga T, Tanaka C, et al. An improved mouse model that rapidly develops fibrosis in non-alcoholic steatohepatitis. Int J Exp Pathol. 2013;94:93-103. doi:10.1111/iep.12008.

23. Thoolen B, Maronpot RR, Harada T, Nyska A, Rousseaux C, Nolte T, et al. Proliferative and Nonproliferative lesions of the rat and mouse hepatobiliary system. Toxicol Pathol. 2010;38:5S-81S. doi:10.1177/0192623310386499. PubMed PMID: 21191096.
24. Suzuki N, Shichiri M, Akashi T, Sato K, Sakurada M, Hirono Y, et al. Systemic distribution of salusin expression in the rat. Hypertens Res. 2007;30:1255. doi:10.1291/hypres.30.1255.
25. Matsuzaka T, Shimano H, Yahagi N, Kato T, Atsumi A, Yamamoto T, et al. Crucial role of a long-chain fatty acid elongase, Elovl6, in obesity-induced insulin resistance. Nature medicine. 2007;13:1193-202. Epub 2007/10/02. doi:10.1038/nm1662. PubMed PMID: 17906635.
26. Ozaki H, Nakano Y, Sakamaki H, Yamanaka H, Nakai M. Basic eluent for rapid and comprehensive analysis of fatty acid isomers using reversed-phase high performance liquid chromatography/Fourier transform mass spectrometry. J Chromatogr A. 2019;1585:113-20. Epub 2019/01/02. doi:10.1016/j.chroma.2018.11.057. PubMed PMID: 30598291.
27. Wakame K, Komatsu KI, Nakata A, Sato K, Takaguri A, Masutomi H, et al. Transcriptome analysis of skin from SMP30/GNL knockout mice reveals the effect of ascorbic acid deficiency on skin and hair. In vivo. 2017;31:599-607. Epub 2017/06/28. doi:10.21873/invivo.11100. PubMed PMID: 28652426; PubMed Central PMCID: PMCPMC5566909.
28. Nakae D, Mizumoto Y, Andoh N, Tamura K, Horiguchi K, Endoh T, et al. Comparative changes in the liver of female Fischer-344 rats after short-term feeding of a semipurified or a semisynthetic L-amino acid-defined choline-deficient diet. Toxicol Pathol. 1995;23:583-90. Epub 1995/09/01. doi:10.1177/019262339502300504. PubMed PMID: 8578101.
29. Kakehashi A, Kato A, Inoue M, Ishii N, Okazaki E, Wei M, et al. Cytokeratin 8/18 as a new marker of mouse liver preneoplastic lesions. Toxicol Appl Pharm. 2010;242:47-55. Epub 2009/10/03. doi:10.1016/j.taap.2009.09.013. PubMed PMID: 19796649.
30. Thapaliya S, Wree A, Povero D, Inzaugarat ME, Berk M, Dixon L, et al. Caspase 3 inactivation protects against hepatic cell death and ameliorates fibrogenesis in a diet-induced NASH model. Digest Dis Sci. 2014;59:1197-206. Epub 2014/05/06. doi:10.1007/s10620-014-3167-6. PubMed PMID: 24795036; PubMed Central PMCID: PMCPMC4512760.
31. Luedde T, Schwabe RF. NF-κB in the liver—linking injury, fibrosis and hepatocellular carcinoma. Nat Rev Gastro Hepat. 2011;8:108. doi:10.1038/nrgastro.2010.213.
32. Li L, He D, Wilborn TW, Falany JL, Falany CN. Increased SULT1E1 activity in HepG2 hepatocytes decreases growth hormone stimulation of STAT5b phosphorylation. Steroids. 2009;74:20-9. Epub 2008/10/04. doi:10.1016/j.steroids.2008.09.002. PubMed PMID: 18831980; PubMed Central PMCID: PMCPMC2633718.
33. Mendez-Sanchez N, Cruz-Ramon VC, Ramirez-Perez OL, Hwang JP, Barranco-Fragoso B, Cordova-Gallardo J. New aspects of lipotoxicity in nonalcoholic steatohepatitis. Int J Mol Sci. 2018;19:2034. PubMed PMID: doi:10.3390/ijms19072034.
34. Marra F, Svegliati-Baroni G. Lipotoxicity and the gut-liver axis in NASH pathogenesis. J Hepatol. 2018;68:280-95. doi:10.1016/j.jhep.2017.11.014.

35. Dhibi M, Brahmi F, Mnari A, Houas Z, Chargui I, Bchir L, et al. The intake of high fat diet with different trans fatty acid levels differentially induces oxidative stress and non alcoholic fatty liver disease (NAFLD) in rats. Nutr Metab. 2011;8:65. doi:10.1186/1743-7075-8-65.
36. Yamada K, Mizukoshi E, Sunagozaka H, Arai K, Yamashita T, Takeshita Y, et al. Characteristics of hepatic fatty acid compositions in patients with nonalcoholic steatohepatitis. Liver Int. 2015;35:582-90. Epub 2014/09/16. doi:10.1111/liv.12685. PubMed PMID: 25219574.
37. Puri P, Baillie RA, Wiest MM, Mirshahi F, Choudhury J, Cheung O, et al. A lipidomic analysis of nonalcoholic fatty liver disease. Hepatology. 2007;46:1081-90. Epub 2007/07/27. doi:10.1002/hep.21763. PubMed PMID: 17654743.
38. Malmsten CL. Prostaglandins, thromboxanes, and leukotrienes in inflammation. Am J Med. 1986;80:11-7. Epub 1986/04/28. PubMed PMID: 2871754.
39. Samuelsson B. Leukotrienes: mediators of immediate hypersensitivity reactions and inflammation. Science. 1983;220:568-75. doi:10.1126/science.6301011.
40. Kuehl F, Egan R. Prostaglandins, arachidonic acid, and inflammation. Science. 1980;210:978-84. doi:10.1126/science.6254151.
41. Nakae D, Kotake Y, Kishida H, Hensley KL, Denda A, Kobayashi Y, et al. Inhibition by phenyl N-tert-butyl nitrone of early phase carcinogenesis in the livers of rats fed a choline-deficient, L-amino acid-defined diet. Cancer Res. 1998;58:4548-51. Epub 1998/10/27. PubMed PMID: 9788598.
42. Jeyapal S, Putcha UK, Mullapudi VS, Ghosh S, Sakamuri A, Kona SR, et al. Chronic consumption of fructose in combination with trans fatty acids but not with saturated fatty acids induces nonalcoholic steatohepatitis with fibrosis in rats. Eur J Nutr. 2018;57:2171-87. doi:10.1007/s00394-017-1492-1.
43. Drescher HK, Weiskirchen R, Fulop A, Hopf C, de San Roman EG, Huesgen PF, et al. The influence of different fat sources on steatohepatitis and fibrosis development in the western diet mouse model of non-alcoholic steatohepatitis (NASH). Front Physiol. 2019;10:770. Epub 2019/07/12. doi:10.3389/fphys.2019.00770. PubMed PMID: 31293441; PubMed Central PMCID: PMCPMC6603084.
44. Jacome-Sosa MM, Borthwick F, Mangat R, Uwiera R, Reaney MJ, Shen J, et al. Diets enriched in trans-11 vaccenic acid alleviate ectopic lipid accumulation in a rat model of NAFLD and metabolic syndrome. J Nutr Biochem. 2014;25:692-701. Epub 2014/04/30. doi:10.1016/j.jnutbio.2014.02.011. PubMed PMID: 24775093.
45. Pfaffenbach KT, Gentile CL, Nivala AM, Wang D, Wei Y, Pagliassotti MJ. Linking endoplasmic reticulum stress to cell death in hepatocytes: roles of C/EBP homologous protein and chemical chaperones in palmitate-mediated cell death. American journal of physiology Endocrinol Metabol. 2010;298:E1027-35. Epub 2010/02/18. doi:10.1152/ajpendo.00642.2009. PubMed PMID: 20159858; PubMed Central PMCID: PMCPMC2867372.
46. Amano Y, Shimizu F, Yasuno H, Harada A, Tsuchiya S, Isono O, et al. Non-alcoholic steatohepatitis-associated hepatic fibrosis and hepatocellular carcinoma in a combined mouse model of genetic

modification and dietary challenge. Hepatol Res. 2017;47:103-15. Epub 2016/03/20. doi:10.1111/hepr.12709. PubMed PMID: 26992446.

47. Cazanave SC, Gores GJ. Mechanisms and clinical implications of hepatocyte lipoapoptosis. Clin Lipidol. 2010;5:71-85. Epub 2010/04/07. doi:10.2217/clp.09.85. PubMed PMID: 20368747; PubMed Central PMCID: PMCPMC2847283.
48. Luedde T, Beraza N, Kotsikoris V, van Loo G, Nenci A, De Vos R, et al. Deletion of NEMO/IKKgamma in liver parenchymal cells causes steatohepatitis and hepatocellular carcinoma. Cancer Cell. 2007;11:119-32. Epub 2007/02/13. doi:10.1016/j.ccr.2006.12.016. PubMed PMID: 17292824.
49. Song WC. Biochemistry and reproductive endocrinology of estrogen sulfotransferase. Ann N Y Acad Sci. 2001;948:43-50. Epub 2002/01/25. PubMed PMID: 11795394.
50. Li L, Falany CN. Elevated hepatic SULT1E1 activity in mouse models of cystic fibrosis alters the regulation of estrogen responsive proteins. J Cys Fibros. 2007;6:23-30. Epub 2006/06/27. doi:10.1016/j.jcf.2006.05.001. PubMed PMID: 16798114.
51. Falany JL, Greer H, Kovacs T, Sorscher EJ, Falany CN. Elevation of hepatic sulphotransferase activities in mice with resistance to cystic fibrosis. Biochem J. 2002;364:115-20. Epub 2002/05/04. PubMed PMID: 11988083; PubMed Central PMCID: PMCPMC1222552.
52. Matsushita N, Hassanein MT, Martinez-Clemente M, Lazaro R, French SW, Xie W, et al. Gender difference in NASH susceptibility: Roles of hepatocyte Ikkbeta and Sult1e1. PloS one. 2017;12:e0181052. Epub 2017/08/11. doi:10.1371/journal.pone.0181052. PubMed PMID: 28797077; PubMed Central PMCID: PMCPMC5552280.
53. Takahashi Y. The role of growth hormone and insulin-like growth factor-I in the liver. Int J Mol Sci. 2017;18. Epub 2017/07/06. doi:10.3390/ijms18071447. PubMed PMID: 28678199; PubMed Central PMCID: PMCPMC5535938.
54. Nishizawa H, Iguchi G, Fukuoka H, Takahashi M, Suda K, Bando H, et al. IGF-I induces senescence of hepatic stellate cells and limits fibrosis in a p53-dependent manner. Scientific reports. 2016;6:34605. doi:10.1038/srep34605 https://www.nature.com/articles/srep34605#supplementary-information.
55. Takahashi Y, Iida K, Takahashi K, Yoshioka S, Fukuoka H, Takeno R, et al. Growth hormone reverses nonalcoholic steatohepatitis in a patient with adult growth hormone deficiency. Gastroenterology. 2007;132:938-43. Epub 2007/02/28. doi:10.1053/j.gastro.2006.12.024. PubMed PMID: 17324404.
56. Nishizawa H, Takahashi M, Fukuoka H, Iguchi G, Kitazawa R, Takahashi Y. GH-independent IGF-I action is essential to prevent the development of nonalcoholic steatohepatitis in a GH-deficient rat model. Biochem Biophys Res Commun. 2012;423:295-300. Epub 2012/06/05. doi:10.1016/j.bbrc.2012.05.115. PubMed PMID: 22659415.

Figures

Figure 1

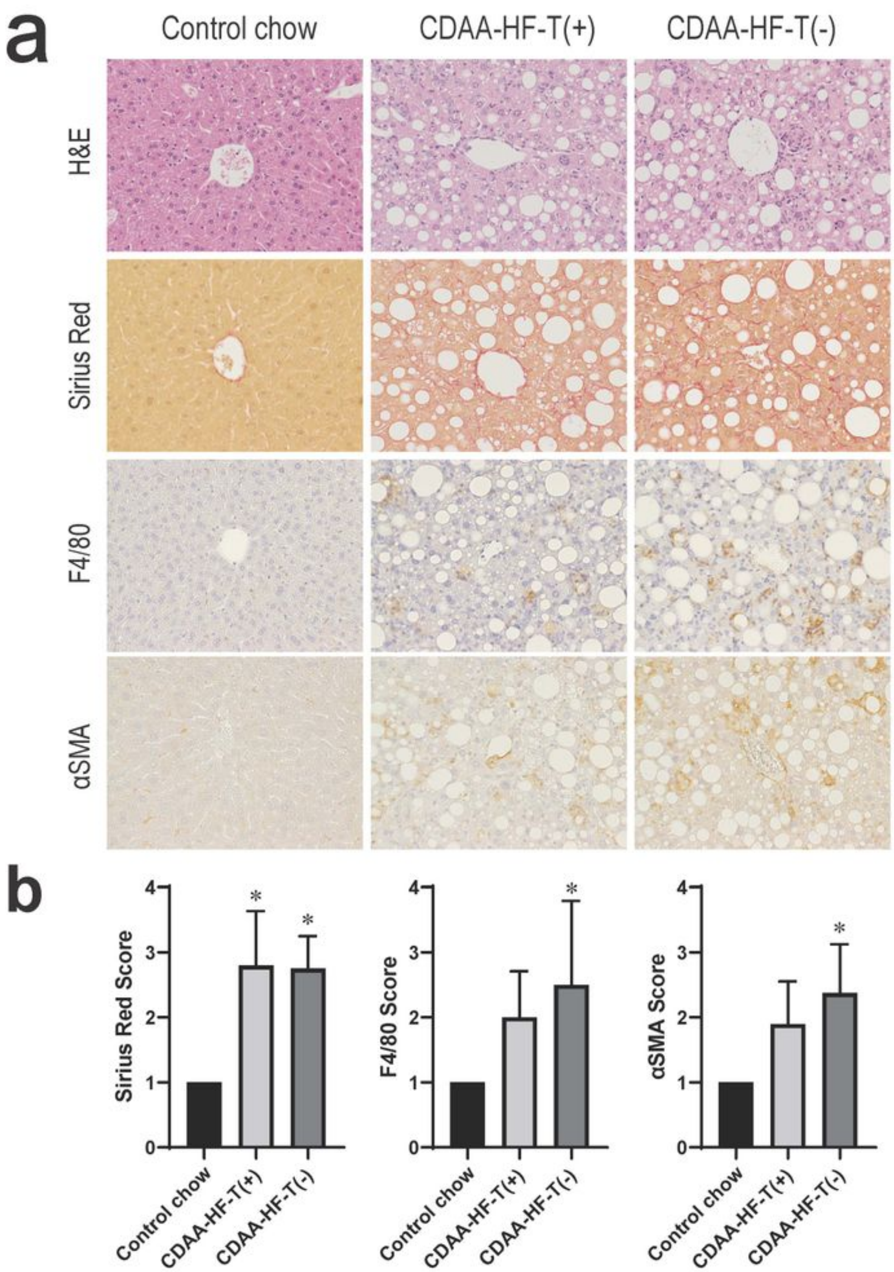

Figure 1

Nonproliferative liver lesions. Histopathological features of H&E and Sirius Red staining and F4/80- and α-SMA-immunohistochemistry (a). Graded from normal (1) to severe (4) (b). *Significantly different from the control value.

Figure 2

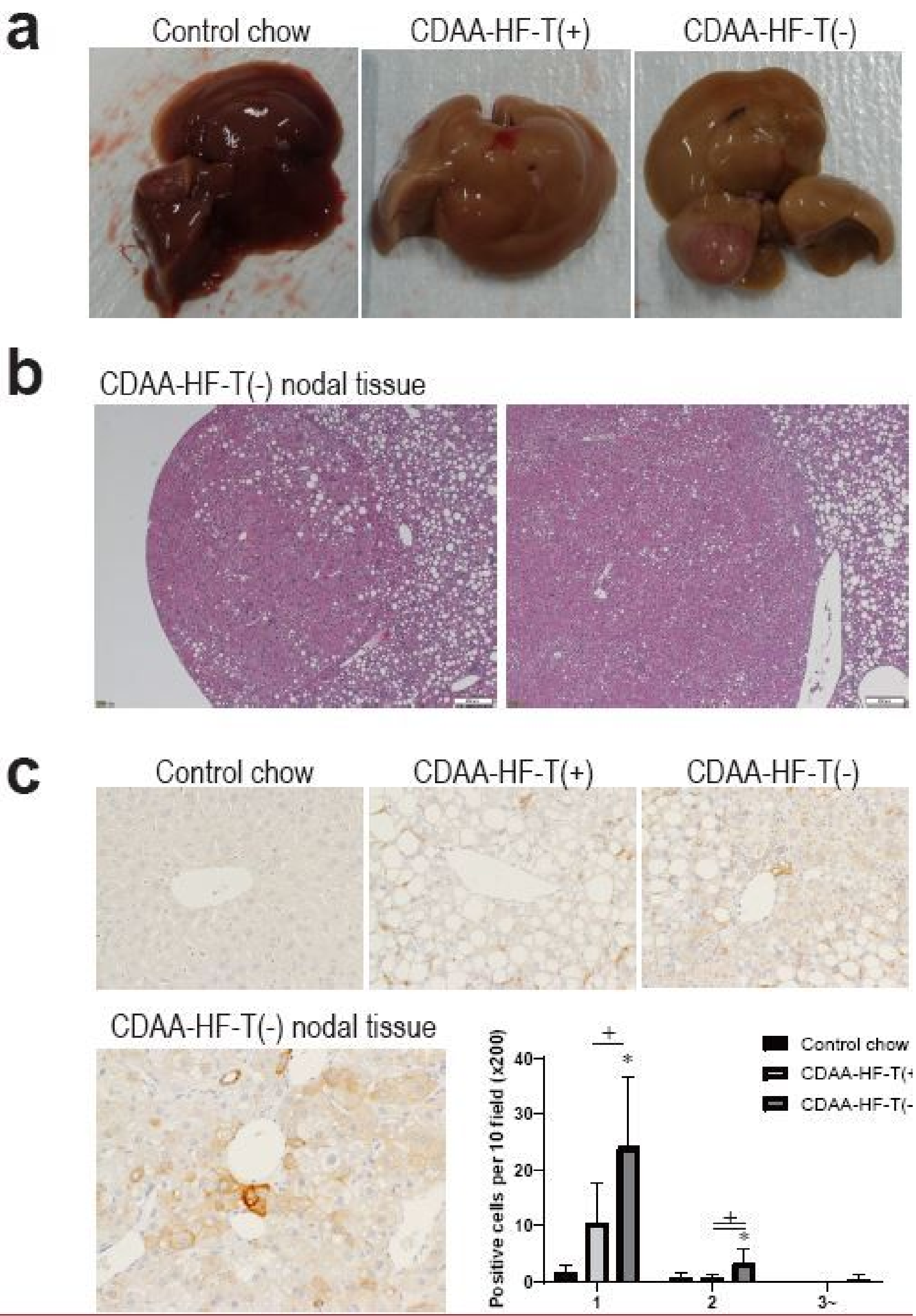

Figure 2

Proliferative liver lesions at the end of week 26. Macroscopic features of the liver from mice (a). Microscopic features (hepatocellular hyperplasia and adenoma) of hepatic proliferative lesions of mice fed the CDAA-HF-T(−) diet (b). The number of CK8/18-positive, putative hepatocellular preneoplastic lesions (c). *Significantly different from the control value. versus chow group; +Significantly different from the CDAA-HF-T(+) value.

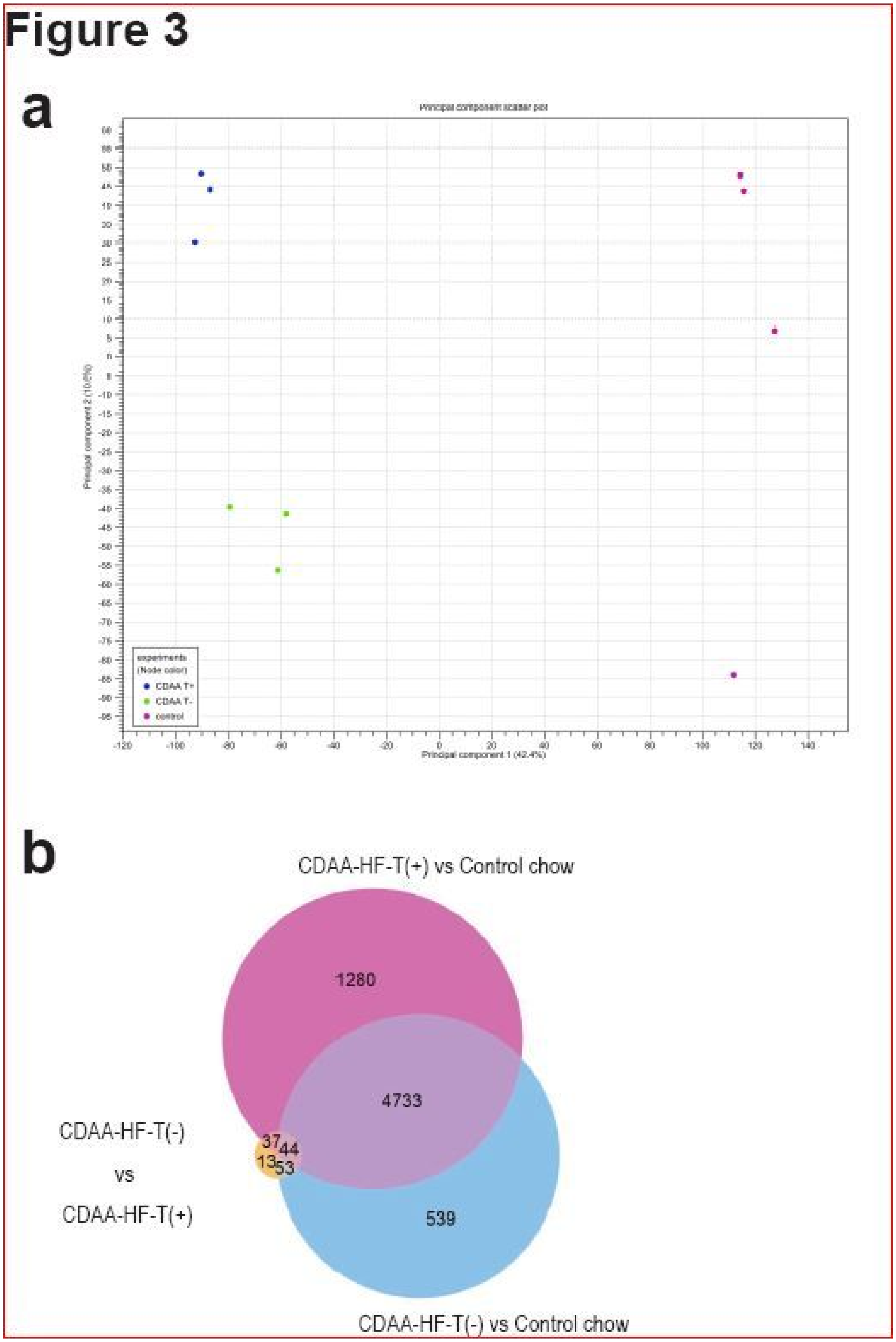

Figure 3

Gene expression profile at the end of week 13. Two-dimensional plot of the principal component analysis for RNA-Seq (a). Venn diagram of the comparison of differentially expressed genes (DEGs) based on RNA-Seq data (b).

Figure 4

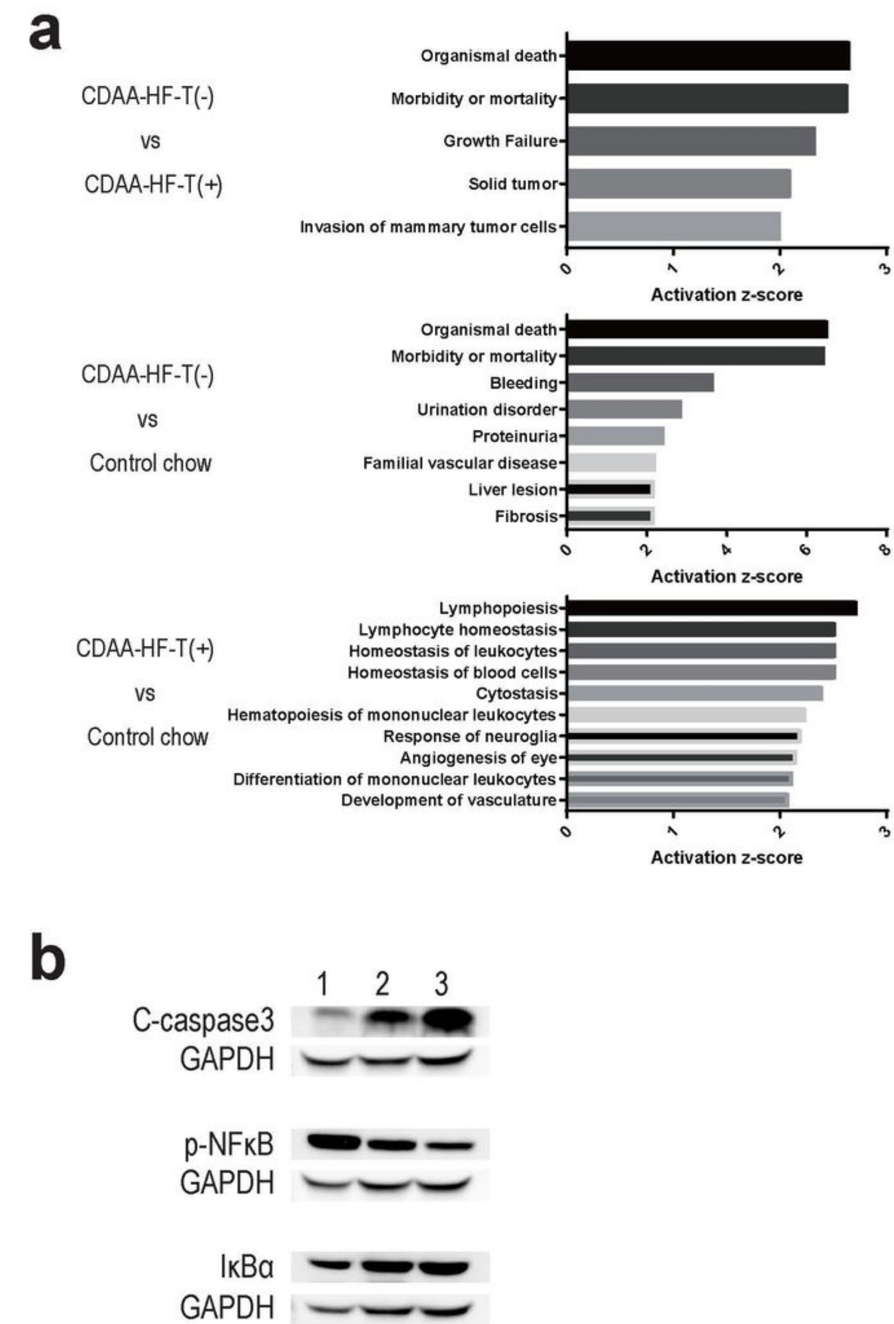

Figure 4

Pathway analysis and hepatic status of apoptosis and NF-κB signaling at the end of week 13. The genes were selected by expression analysis for comparisons between the control, CDAA-HF-T(+), and CDAA-HF-T(−) groups, with an FDR p value <0.05 and/or FC >±1.5. Activated disease or functional annotation (|z-score| >=2) for DEGs in Ingenuity Pathway Analysis (a). Densitometric outcomes of the immunoblot analyses of cleaved caspase 3 and phosphorylated NF-κB and I-κBα levels expressed as the ratios versus the GAPDH level (b). The control diet (1), CDAA-HF-T(+) (2), and CDAA-HF-T(−) (3) groups.

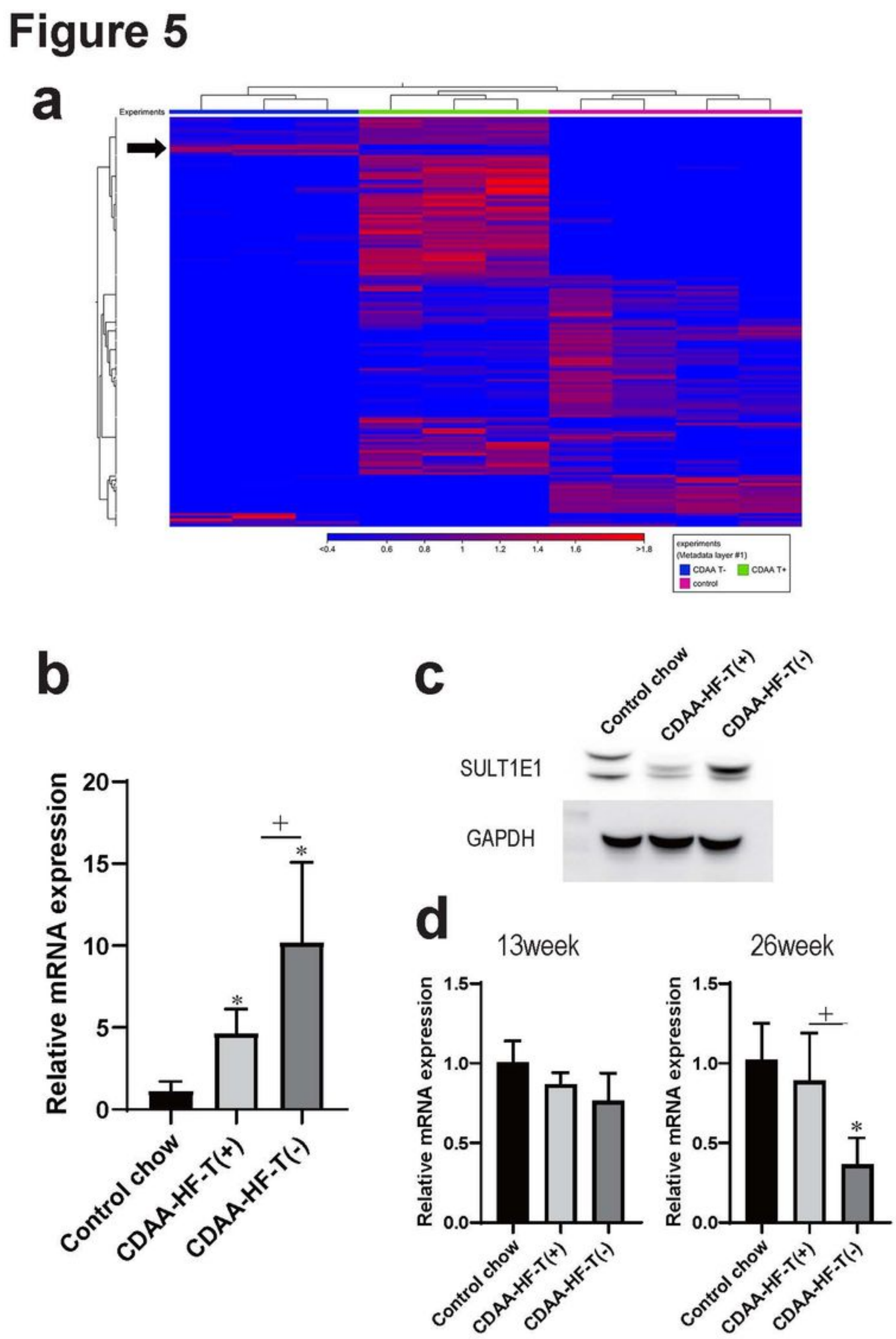

Figure 5

SULT1E1 and IGF-1 expression levels Two-dimensional heat map of the expression values of DEGs where arrows indicate the genes overexpressed only in the CDAA-HF-T(−) group (a). qPCR of the SULT1E1 gene (b). Immunoblot analysis of the SULT1E1 protein (c). qPCR of the IGF-1 gene at the end of weeks 13 and

26 (d). *Significantly different from the control value. +Significantly different from the CDAA-HF-T(+) value.

Supplementary Files

This is a list of supplementary files associated with this preprint. Click to download.

- Additionalfile4.xlsx
- Additionalfile3.pdf
- Additionalfile2.pdf
- Additionalfile1.pdf